

# Azo-coupled zinc phthalocyanines: Towards broad absorption and application in dye-sensitized solar cells



Mingliang Han, Xuejun Zhang\*, Xiaoxia Zhang, Chaoqiang Liao, Baiqing Zhu, Qiaoling Li

Department of Chemistry, School of Science, North University of China, Taiyuan 030051, Shanxi Province, PR China

## ARTICLE INFO

### Article history:

Received 14 July 2014

Accepted 11 October 2014

Available online 1 November 2014

### Keywords:

Azobenzene  
Phthalocyanines  
Dye-sensitized solar cells  
Absorption spectra  
Electrochemistry

## ABSTRACT

The synthesis of symmetrical azo-coupled zinc phthalocyanines (**7**, **8**, **10** and **11**) incorporating two spectrally complementary photogenerators (azo dyes and phthalocyanines) by N=N double bonds in a single structure was described. The four sensitizers were fully characterized by Fourier Transform infrared spectroscopy, UV–Vis spectroscopy, proton nuclear magnetic resonance, mass spectrometry, elemental analyses, thermogravimetric analysis and cyclic voltammetry. All the azo-coupled phthalocyanines exhibited broad absorptions covering the range 300–800 nm. The cyclic voltammetry studies indicated that the LUMO and HOMO energy levels of four synthesized azo-coupled phthalocyanines could ensure efficient electron injection and thermodynamically favorable dye regeneration. Thermal stability studies showed that the four sensitizers were stable above 200 °C. The new compounds were tested in dye-sensitized solar cells and compound **8** showed the best photovoltaic performance, yielding 2.7% power conversion efficiency.

© 2014 Elsevier Ltd. All rights reserved.

## 1. Introduction

Dye-sensitized solar cells (DSSCs) based on dye sensitized nanocrystalline TiO<sub>2</sub> photoelectrodes have received considerable attention due to their low cost, decorative nature, ease of fabrication, short energy pay-back time and being more environmentally pleasant than conventional solar cells based on inorganic silicon semiconductors [1,2]. A typical DSSC is composed of a photo-anode (consisting of a fluorine-doped SnO<sub>2</sub> glass substrate, a nanocrystalline TiO<sub>2</sub> thin film and dye sensitizers) and a Pt-doped photoinert counter electrode (cathode), sandwiching a redox mediator. To date, power conversion efficiencies of more than 9% have been achieved for state-of-the-art DSSCs [3,4]. The performances of DSSCs are mainly correlated with the properties of the sensitizers. Organic sensitizers with higher LUMO energy levels, smaller energy gaps and wide wavelength range absorption bands will be superb [3].

Phthalocyanines (Pcs) and their metal complexes, as planar two-dimensional aromatics, are typical NIR dyes [5]. Pcs have strong absorptions on two distinct edges of the visible region, namely the Q-band at around 700 nm and the Soret-band at around 350 nm. These macrocycles, in combination with other electro- and photoactive moieties, have been ideal building blocks

for the construction of molecular materials with designed electronic and optical properties [3,6]. Additionally, the facile modification of the chromophore skeleton of phthalocyanines provides potential for molecular design. Based on these attributes, phthalocyanines are rendered attractive for the potential application in dye-sensitized solar cells (DSSC) [7–11].

Up until now, various chromophores have been introduced into the phthalocyanine core to tune the absorption over a broad spectral range and to achieve high extinction coefficients, including coumarin derivatives [12], azo dyes [13–15], triphenylamine groups [10], thienyls [16], multicomponent systems such as tetra-thiafulvalenes [17], fluorenyl [18] and perylenediimide [19]. However, we found that almost all the chromophores were introduced through oxygen bridges [12–15], thioether bonds [20] or C–C bonds [7,10], and the characteristic absorptions of these chromophores overlapped with the Soret-band of the phthalocyanines. Moreover, the absorption bands of these phthalocyanines red shifted slightly. Also, for Pc dyes, the spectral window between 400 and 600 nm still exhibited almost no absorptions [19]. In order to overcome the problems mentioned above, azo dyes were chosen as chromophores and these were connected onto the Pc ring through the N=N double bond. Pcs and azo dyes show great attractiveness due to their broad availability and perfectly complementary absorption regions. Azo compounds are the oldest and largest class of industrial synthesized organic dyes due to their versatile application in the fields of dyes and pigments [21–23].

\* Corresponding author. Tel./fax: +86 351 3922152.

E-mail address: [zhangxuejun@nuc.edu.cn](mailto:zhangxuejun@nuc.edu.cn) (X. Zhang).

Nowadays, azo dyes have been deeply investigated and applied in high technology areas due to their idiosyncratic optical properties, such as optical information storage [24], liquid crystalline displays [25] and non-linear optics [26]. Azo dyes show intense absorptions in the visible region (400–650 nm) and always have two absorption bands corresponding to the long wavelength generated by the  $n \rightarrow \pi^*$  transition and the short wavelength generated by the  $\pi \rightarrow \pi^*$  transition.

Herein, we designed and synthesized four symmetrical azo-coupled zinc phthalocyanines with hydroxyl and carboxyl as anchoring groups, which incorporated two spectrally complementary photogenerators (azo dyes and Pcs) by N=N double bonds in single structures. The new compounds showed wide and intense absorption bands in the whole visible region and some of the near-infrared region. To the best of our knowledge, reports on phthalocyanine–azobenzene dyads bearing anchoring groups, such as panchromatic and functional molecules, and their application in dye-sensitized solar cells are still scarce. In this manuscript, the synthesis, characterization, spectroscopic, electrochemistry, thermal studies and TiO<sub>2</sub> photoelectrode tests of four azo-coupled zinc phthalocyanines were reported.

## 2. Experimental

### 2.1. Materials and equipment

#### 2.1.1. Materials

Fe powders, 4-nitrophthalonitrile, phenol, 1-naphthalenol, 4-hydroxybenzoic acid, p-aminobenzoic acid, sodium hydroxide, sodium nitrite, zinc acetate dihydrate, tetrabutylammonium perchlorate, vanilline and 1,8-diazabicyclo [5.4.0]-undec-7-ene (DBU) were purchased from Aladdin. Methanol, acetone, acetic acid, chloroform, n-pentanol, ethyl acetate, N,N-dimethylformamide (DMF), dimethyl sulfoxide (DMSO) and tetrahydrofuran (THF) were purchased from Damao reagent company. All reagents and solvents were analytical grade. All solvents were dried and purified as described by Perin and Armarego [27]. 4-Hydroxybenzoate was prepared from 4-hydroxybenzoic acid according to classical procedures. Column chromatography was performed on silica gel (80–100 mesh).

#### 2.1.2. Equipment

Infrared spectra (IR) were recorded on a Shimadzu 4800S Fourier Transform Infrared spectrophotometer using KBr pellets. <sup>1</sup>H NMR spectra were obtained in DMSO-d<sub>6</sub> solvent using a Bruker DRX 300 MHz NMR spectrometer, and chemical shifts are reported relative to tetramethylsilane (TMS) as an internal reference. The UV–Vis spectra were recorded with a Techcomp 2300 spectrophotometer. Elemental analyses were performed on a Flash EA1112 elemental analyzer (C, H, N). MALDI-TOF mass spectrometric measurements were performed on a Bruker Biflex III MALDI-TOF. Thermogravimetric measurements were carried out on a ZCT-A instrument with a heating rate of 10 °C min<sup>-1</sup> under nitrogen.

The current–voltage characteristics of the cells were measured on a computer-controlled voltage–current source meter (Advantest, R6243) under illumination of simulated AM1.5G solar light from an AM1.5 solar simulator (Wacom Co., WXS-80C-3 with a 450 W xenon lamp). The incident light intensity was calibrated by using a standard mono-Si solar cell, giving the photoresponse range of an amorphous silicon solar cell. The standard solar cell was produced and calibrated by the Japan Quality Assurance Organization.

Cyclic voltammetry measurements were performed on an electrochemical workstation (CHI LK2005A, Tianjin Lanlike Chemistry electronic high-tech Co., Ltd., PR China). A three electrode set-up

was employed, consisting of a platinum wire as the working electrode, another platinum wire as the counter film electrode and a standard calomel electrode (SCE) as the reference electrode. The dyes were analyzed in dry THF containing tetrabutylammonium perchlorate (0.1 M) as the supporting electrolyte.

### 2.2. Device fabrication

The screen-printing method was used to prepare the TiO<sub>2</sub> photoelectrodes, as reported in the literature [28,29]. The 10 wt% P25 TiO<sub>2</sub> nanoparticles were well dispersed in ethanol, and then the dispersed solution was electrospayed through a plastic syringe, that had a metallic microtip connected to a high-voltage power supply, onto a washed transparent conducting glass (which had been coated with a fluorine-doped stannic oxide layer, with a thickness of 4 mm and sheet resistance of 18–20 Ω). Subsequently, the as-prepared TiO<sub>2</sub> spheres were placed between two steel plates and laminated under a pressure of 12 MPa. The pressed TiO<sub>2</sub> films were dried at 150 °C for 30 min and then were gradually sintered at 500 °C for 20 min to fabricate the photoelectrode layers. The sensitizers **7**, **8**, **10** and **11** were dissolved in THF at a concentration of  $1 \times 10^{-4}$  M. The TiO<sub>2</sub> films were immersed into the dye solutions and then kept at room temperature for 15 h so that the dyes were adsorbed onto the TiO<sub>2</sub> films. Then, the dye-adsorbed photoelectrodes were washed with THF and ethanol to remove non-adsorbed dyes under a stream of nitrogen. The dye-sensitized electrodes were assembled and sealed with the Pt-CEs using hot-melt ionomer adhesive films (Surlyn, 25 μm thickness, DuPont 1702) to acquire a gap between the two electrodes. The Pt-CE was prepared from hexachloroplatinic acid by chemical deposition. The electrolyte prepared from 0.05 M iodine and 0.5 M LiI in acetonitrile was introduced through the pre-drilled hole. The holes were then covered with a glass cover. Photoelectrochemical data were tested with a 450 W xenon light source, focused to give 1000 W/m<sup>2</sup>, the equivalent of one sun at AM 1.5, at the surface of the test cells. In order to reduce scattered light from the edge of the glass electrodes of the dyed TiO<sub>2</sub> layer, a light-shading mask was also used on the devices.

### 2.3. Synthesis

#### 2.3.1. 4-Aminophthalonitrile (**1**)

A mixture of Fe powders (2.05 g, 33.60 mmol) and concentrated hydrochloric acid (1 ml) in deionized water (50 ml) was heated and stirred at 60 °C for 30 min. Then 4-nitrophthalonitrile (2.00 g, 11.56 mmol) was added portionwise over a period of 60 min. After the addition of the 4-nitrophthalonitrile, the temperature was raised to 75 °C and the mixture was stirred vigorously for a further 1.5 h. The reaction mixture was then filtered through a Büchner funnel. The residues were washed with 150 ml hot methanol. Washings were concentrated and the obtained faint yellow precipitate was filtered off, washed with water until the washings were neutral. The white pure product was recovered by recrystallization using methanol. Yield: 1.07 g (65%). M.p.: 179–181 °C. Anal. Calc. for C<sub>8</sub>H<sub>5</sub>N<sub>3</sub>: C, 67.13; H, 3.49; N, 29.37. Found: C, 67.09; H, 3.46; N, 29.28%. FT-IR (KBr tablet)  $\nu_{\max}$ , cm<sup>-1</sup>: 3452, 3354 (N–H), 3079 (Ar–H), 2220 (C≡N), 1598 (C=C), 1332 (C–N), 1638, 1494, 1256.

#### 2.3.2. 4-(4-Hydroxyphenylazo)phthalonitrile (**2**)

**2.3.2.1. Diazotization.** A mixture of **1** (1.43 g, 10 mmol) and concentrated hydrochloric acid (3 ml) in deionized water (30 ml) was stirred in an ice bath until blended well. Then a solution of sodium nitrite (0.76 g, 11 mmol) was added dropwise to the slurry-like mixture at 0–5 °C over about 20 min. The stirring was continued for another 30 min, then the reaction mixture was filtered, and the bright yellow solution was kept in an ice bath for the next step.

**2.3.2.2. Coupling.** The prepared diazonium salt solution was slowly added to a stirred solution of phenol (0.94 g, 10 mmol) as the coupling component in alkali medium by adjusting the pH value to 8–9 using a sodium hydroxide solution (30%) and the temperature was maintained at 0–5 °C. The resulting solution was stirred for 30 min in an ice bath and then allowed to reach room temperature. After 1 h, the pH value of the diazo liquor was adjusted to 3–4 by adding a diluted hydrochloric acid solution. The precipitated jacinth solids were filtered off, washed several times with cold water and purified by further recrystallization from acetone and finally dried under vacuum at 60 °C overnight. Yield: 1.76 g (71%). M.p.: 223–225 °C. *Anal. Calc.* for  $C_{14}H_8N_4O_2$ : C, 67.74; H, 3.22; N, 22.58. Found: C, 67.64; H, 3.25; N, 22.53%. UV–Vis (THF)  $\lambda_{max}$ , nm (log  $\epsilon$ ): 378 (4.82), 489 (4.03). FT-IR (KBr tablet)  $\nu_{max}$ ,  $cm^{-1}$ : 3339 (O–H), 3033 (Ar–H), 2242 (C≡N), 1601, 1581 (C=C), 1460 (N=N), 1505, 1420, 1392, 1352, 1290, 1202, 1135.  $^1H$  NMR (DMSO- $d_6$ )  $\delta$ , ppm: 10.41 (1H, s, OH), 8.41 (1H, d, Ar–H), 8.34 (1H, s, Ar–H), 7.84 (1H, d, Ar–H), 7.75 (2H, d, Ar–H), 6.91 (2H, d, Ar–H).

### 2.3.3. 4-(4-Hydroxynaphthalen-1-ylazo)phthalonitrile (3)

**2.3.3.1. Diazotization.** The same procedure and molar ratio of the reagents given in section 2.3.2.1 were followed.

**2.3.3.2. Coupling.** The prepared diazonium salt solution was slowly added to a stirred solution of 1-naphthalenol (1.44 g, 10 mmol) in alkali medium by adjusting the pH value to 8–9 using a sodium hydroxide solution (30%) and the temperature was maintained at 0–5 °C. The resulting solution was stirred for 30 min in an ice bath and after another 30 min the pH value of the diazo liquor was adjusted to 3–4 by adding a diluted hydrochloric acid solution. The precipitated red solids were filtered off, washed several times with cold water and purified by further recrystallization from acetic acid and finally dried under vacuum at room temperature for 2 days. Yield: 1.87 g (63%). M.p.: 292–295 °C. *Anal. Calc.* for  $C_{18}H_{10}N_4O$ : C, 72.48; H, 3.35; N, 18.79. Found: C, 72.41; H, 3.33; N, 18.72%. UV–Vis (THF)  $\lambda_{max}$ , nm (log  $\epsilon$ ): 308 (4.46), 453 (4.83), 607 (3.98). FT-IR (KBr tablet)  $\nu_{max}$ ,  $cm^{-1}$ : 3259 (O–H), 3079 (Ar–H), 2226 (C≡N), 1595 (C=C), 1482 (N=N), 1414, 1361, 1310, 1256, 1183, 758.  $^1H$  NMR (DMSO- $d_6$ )  $\delta$ , ppm: 10.27 (1H, s, OH), 8.42 (1H, d, Ar–H), 8.37 (1H, s, Ar–H), 8.08 (1H, d, Ar–H), 7.91 (1H, d, Ar–H), 7.84 (1H, d, Ar–H), 7.68 (1H, d, Ar–H), 7.38 (1H, m, Ar–H), 7.35 (1H, m, Ar–H), 6.89 (1H, d, Ar–H).

### 2.3.4. 4-(2-Hydroxy-5-ethyl-oxycarbonyl-phenylazo) phthalonitrile (4)

**2.3.4.1. Diazotization.** The same procedure and molar ratio of the reagents given in section 2.3.2.1 were followed.

**2.3.4.2. Coupling.** The prepared diazonium salt solution was slowly added to a stirred solution of ethyl 4-hydroxybenzoate (1.66 g, 10 mmol) in alkali medium by adjusting the pH value to 8–9 using sodium hydroxide (30%) solution and the temperature was maintained at 0–5 °C. The resulting solution was stirred for 30 min in an ice bath and then allowed to reach room temperature. After 1 h, the pH value of the diazo liquor was adjusted to 3–4 by adding diluted hydrochloric acid solution. The precipitated brown orange solids were filtered off, washed several times with cold water and purified by further recrystallization from acetone and finally dried under vacuum at 60 °C overnight. Yield: 2.17 g (68%). M.p.: 183–185 °C. *Anal. Calc.* for  $C_{17}H_{12}N_4O_3$ : C, 63.75; H, 3.75; N, 17.5. Found: C, 63.69; H, 3.73; N, 17.52%. UV–Vis (THF)  $\lambda_{max}$ , nm (log  $\epsilon$ ): 378 (4.80), 488 (4.01). FT-IR (KBr tablet)  $\nu_{max}$ ,  $cm^{-1}$ : 3221 (O–H), 3067 (Ar–H), 2984–2903 (Aliph. C–H), 2236 (C≡N), 1708 (C=O), 1615, 1587 (C=C), 1446 (N=N), 1395, 1369, 1287, 1239, 1171.  $^1H$  NMR (DMSO- $d_6$ )  $\delta$ , ppm: 9.44 (1H, s, OH), 8.39 (1H, d, Ar–H), 8.36 (1H, d, Ar–H), 7.89 (1H, d, Ar–H), 7.87 (1H, d, Ar–H), 7.73

(1H, d, Ar–H), 7.64 (1H, s, Ar–H), 4.29 (2H, m, Aliph. C–H), 1.30 (3H, m, Aliph. C–H).

### 2.3.5. 4-[(4-Hydroxy-3-methoxybenzylidene)amino]benzoic acid (5)

A mixture of vanilline (2.28 g, 15 mmol) and ethyl 4-aminobenzoic acid (2.47 g, 15 mmol) in ethanol (30 ml) was refluxed under a nitrogen atmosphere until the starting material could no longer be detected by TLC. After the reaction completed, the solvent was evaporated and the yellow crude product was purified by silica gel chromatography column with chloroform alone as the eluent. The title compound was dried under vacuum at 60 °C overnight. Yield: 3.41 g (76%). M.p.: 142–146 °C. *Anal. Calc.* for  $C_{15}H_{13}NO_4$ : C, 66.42; H, 4.79; N, 5.16. Found: C, 66.49; H, 4.72; N, 5.18%. UV–Vis (THF)  $\lambda_{max}$ , nm (log  $\epsilon$ ): 326 (4.68), 427 (3.72). FT-IR (KBr tablet)  $\nu_{max}$ ,  $cm^{-1}$ : 3508 (O–H), 3079 (Ar–H), 2991–2862 (Aliph. C–H), 1683 (C=O), 1593 (C=N), 1511, 1427, 1320, 1204, 1167.  $^1H$  NMR (DMSO- $d_6$ )  $\delta$ , ppm: 12.56 (1H, s, COOH), 9.57 (1H, s, OH), 8.13 (2H, d, Ar–H), 7.49 (2H, d, Ar–H), 8.35 (1H, s, CH=N), 7.01 (1H, d, Ar–H), 6.96 (1H, s, Ar–H), 6.65 (1H, d, Ar–H), 3.73 (3H, s, Aliph. C–H).

### 2.3.6. 4-[2-Hydroxy-3-methoxy-4-(4-carboxy-benzylidene-amino)phenylazo]phthalonitrile (6)

**2.3.6.1. Diazotization.** The same procedure and molar ratio of the reagents given in section 2.3.2.1 were followed.

**2.3.6.2. Coupling.** The prepared diazonium salt solution was slowly added to a stirred solution of **5** (2.99 g, 10 mmol) in alkali medium by adjusting the pH value to 8–9 using a sodium hydroxide solution (30%) and the temperature was maintained at 0–5 °C. The resulting solution was stirred for 30 min in an ice bath and then allowed to reach room temperature. After 30 min, the pH value of the diazo liquor was adjusted to 3–4 by adding a diluted hydrochloric acid solution. The precipitated reddish brown solids were filtered off, washed several times with cold water, purified by further recrystallization from acetone and finally dried under vacuum at room temperature for 2 days. Yield: 2.33 g (53%). M.p.: 161–164 °C. *Anal. Calc.* for  $C_{23}H_{15}N_5O_4$ : C, 64.94; H, 3.52; N, 16.47. Found: C, 64.87; H, 3.49; N, 16.51%. UV–Vis (THF)  $\lambda_{max}$ , nm (log  $\epsilon$ ): 336 (4.86), 518 (4.17). FT-IR (KBr tablet)  $\nu_{max}$ ,  $cm^{-1}$ : 3374 (O–H), 3077 (Ar–H), 2925 (Aliph. C–H), 2231 (C≡N), 1688 (C=O), 1599 (C=N), 1508 (N=N), 1276, 1022 (C–O–C), 1433, 1386, 1172.  $^1H$  NMR (DMSO- $d_6$ )  $\delta$ , ppm: 12.85 (1H, s, COOH), 10.24 (1H, s, OH), 8.11 (2H, d, Ar–H), 7.5 (2H, d, Ar–H), 8.41 (1H, s, CH=N), 8.44 (1H, d, Ar–H), 7.92 (1H, d, Ar–H), 8.36 (1H, s, Ar–H), 7.68 (1H, s, Ar–H), 7.16 (1H, s, Ar–H), 3.71 (3H, s, Aliph. C–H).

### 2.3.7. Tetrakis-(4-hydroxyphenylazo) phthalocyaninato zinc(II) (7)

A mixture of **2** (1.18 g, 5 mmol), DBU (4 ml, 2.6 mmol) and zinc acetate dihydrate (0.28 g, 1.3 mmol) in n-pentanol (30 ml) was refluxed and stirred under a nitrogen atmosphere for 24 h. Thereafter, methanol (50 ml) was added to the reaction mixture, followed by refluxing for 30 min. The resulting black suspension was filtered off, washed with deionized water, dilute hydrochloric acid, methanol, acetone and ethyl acetate. The black solid after filtration was subjected to Soxhlet extraction using an acetone-methanol (volume ratio 1:1) mixture for 24 h to afford pure **7**. Yield: 0.47 g (36%). M.p.: >300 °C. *Anal. Calc.* for  $C_{56}H_{32}N_{16}O_4Zn$ : C, 62.13; H, 3.02; N, 21.18. Found: C, 62.17; H, 3.05; N, 21.14%. UV–Vis (THF)  $\lambda_{max}$ , nm (log  $\epsilon$ ): 376 (4.78), 649 (4.24), 718 (4.72). MALDI-TOF MS ( $m/z$ ):  $C_{56}H_{32}N_{16}O_4Zn$  [1058.36]:  $M^+$  1058.62. FT-IR (KBr tablet)  $\nu_{max}$ ,  $cm^{-1}$ : 3203 (O–H), 3073 (Ar–H), 1587 (C=C), 1479 (N=N), 1502, 1341, 1274, 1231, 1140, 1091, 841, 745.  $^1H$  NMR (DMSO- $d_6$ )  $\delta$ , ppm: 10.43 (4H, s, OH), 6.96–7.1 (8H, d, Ar–H), 8.93–9.06 (8H, d, Ar–H), 7.85–8.34 (12H, m, Pc ring).

### 2.3.8. Tetrakis-(4-hydroxynaphthalen-1-ylazo)phthalocyaninato zinc(II) (**8**)

The synthesis and purification was as outlined for **7**, except **3** (1.48 g, 5 mmol) was employed instead of **2**. The same molar ratio of the reagents given in section 2.3.7 was followed. Yield: 0.42 g (27%). M.p.: >300 °C. Anal. Calc. for  $C_{72}H_{40}N_{16}O_4Zn$ : C, 68.71; H, 3.18; N, 17.81. Found: C, 68.68; H, 3.16; N, 17.79%. MALDI-TOF MS ( $m/z$ ):  $C_{72}H_{40}N_{16}O_4Zn$  [1258.60]:  $M^+$  1258.41. UV-Vis (THF)  $\lambda_{max}$ , nm (log  $\epsilon$ ): 462 (4.74), 740 (4.77). FT-IR (KBr)  $\nu_{max}$ ,  $cm^{-1}$ : 3367, 3220 (O—H), 3067 (Ar—H), 1598 (C=C), 1488 (N=N), 1544, 1454, 1315, 1248, 1197, 1087, 1050, 838, 764, 747.  $^1H$  NMR (DMSO- $d_6$ )  $\delta$ , ppm: 10.20 (4H, s, OH), 8.08 (4H, d, Ar—H), 7.35–7.38 (8H, m, Ar—H), 7.68 (4H, d, Ar—H), 7.91–8.03 (12H, m, Pc ring), 7.81 (4H, d, Ar—H), 6.88 (4H, d, Ar—H).

### 2.3.9. Tetrakis-(2-hydroxy-5-ethyl-oxycarbonyl-phenylazo)phthalocyaninato zinc(II) (**9**)

The synthesis and purification was as outlined for **7**, except **4** (1.60 g, 5 mmol) was employed instead of **2**. The same molar ratio of the reagents given in section 2.3.7 was followed. Yield: 0.53 g (32%). M.p.: >300 °C. Anal. Calc. for  $C_{68}H_{48}N_{16}O_{12}Zn$ : C, 60.65; H, 3.56; N, 16.64. Found: C, 65.58; H, 3.53; N, 16.59%. MALDI-TOF MS ( $m/z$ ):  $C_{68}H_{48}N_{16}O_{12}Zn$  [1346.54]:  $M^+$  1346.87. UV-Vis (THF)  $\lambda_{max}$ , nm (log  $\epsilon$ ): 361 (4.79), 649 (4.24), 715 (4.70). FT-IR (KBr)  $\nu_{max}$ ,  $cm^{-1}$ : 3361 (O—H), 2932, 2858 (Aliph. C—H), 1703 (C=O), 1598 (C=C), 1494 (N=N), 1559, 1460, 1364, 1282, 1228, 1095, 838, 770, 747.  $^1H$  NMR (DMSO- $d_6$ ) ( $\delta$ : ppm): 9.49 (4H, s, OH), 8.62 (4H, s, Ar—H), 8.14 (4H, d, Ar—H), 7.17 (4H, d, Ar—H), 7.83–7.91 (12H, m, Pc ring), 4.27 (2H, m, Aliph. C—H), 1.27 (3H, m, Aliph. C—H).

### 2.3.10. Tetrakis-(2-hydroxy-5-carboxy-phenylazo)phthalocyaninato zinc(II) (**10**)

A mixture of potassium hydroxide solution (10 ml, 5 mol/L), THF (10 ml) and **9** (0.3 mmol, 0.40 g) was stirred at 75 °C for 6 h. The black green solution was filtered and re-precipitated with dilute hydrochloric acid. The black solid after filtration was subjected to Soxhlet extraction using an acetone-methanol (volume ratio 1:1) mixture for 24 h to afford pure **10**. Yield: 0.24 g (68%). M.p.: >300 °C. Anal. Calc. for  $C_{60}H_{32}N_{16}O_{12}Zn$ : C, 58.37; H, 2.59; N, 18.16. Found: C, 58.31; H, 2.56; N, 18.13%. MALDI-TOF MS ( $m/z$ ):  $C_{60}H_{32}N_{16}O_{12}Zn$  [1234.40]:  $M^+$  1234.69. UV-Vis (THF)  $\lambda_{max}$ , nm (log  $\epsilon$ ): 362 (4.82), 647 (4.37), 716 (4.78). FT-IR (KBr)  $\nu_{max}$ ,  $cm^{-1}$ : 3435, 3248 (O—H), 3039 (Ar—H), 1720 (C=O), 1587 (C=C), 1494 (N=N), 1646, 1440, 1381, 1296, 1185, 1135, 846, 761.  $^1H$  NMR (DMSO- $d_6$ )  $\delta$ , ppm: 12.73 (4H, s, COOH), 9.48 (4H, s, OH), 8.63 (4H, s, Ar—H), 8.16 (4H, d, Ar—H), 7.14 (4H, d, Ar—H), 7.84–7.92 (12H, m, Pc ring).

### 2.3.11. Tetrakis-[2-hydroxy-3-methoxy-4-(4-carboxy-N-phenylmethanimino)phenylazo]phthalocyaninato zinc(II) (**11**)

The synthesis and purification was as outlined for **7**, except **6** (2.21 g, 5 mmol) was employed instead of **2**. The same molar ratio of the reagents given in section 2.3.7 was followed. Yield: 0.54 g (24%). M.p.: >300 °C. Anal. Calc. for  $C_{92}H_{60}N_{20}O_{16}Zn$ : C, 62.53; H, 3.39; N, 15.86. Found: 62.49; H, 3.36; N, 15.89%. MALDI-TOF MS ( $m/z$ ):  $C_{92}H_{60}N_{20}O_{16}Zn$  [1766.99]:  $M^+$  1767.21. UV-Vis (THF)  $\lambda_{max}$ , nm (log  $\epsilon$ ): 664 (4.46), 729 (4.86). FT-IR (KBr)  $\nu_{max}$ ,  $cm^{-1}$ : 3355, 3220 (O—H), 2932, 2858 (Aliph. C—H), 1700 (C=O), 1598 (C=N), 1488 (N=N), 1205, 1050 (C—O—C), 1649, 1559, 1542, 1457, 1140, 1098, 838, 787, 747.  $^1H$  NMR (DMSO- $d_6$ )  $\delta$ , ppm: 12.85 (4H, s, COOH), 10.24 (4H, s, OH), 8.09 (8H, d, Ar—H), 7.49 (8H, d, Ar—H), 8.43 (4H, s, CH=N), 7.38 (4H, s, Ar—H), 7.68 (4H, s, Ar—H), 7.98–8.16 (12H, m, Pc ring), 3.83–3.95 (12H, s, Aliph. C—H).

## 3. Results and discussion

### 3.1. Synthesis and characterization

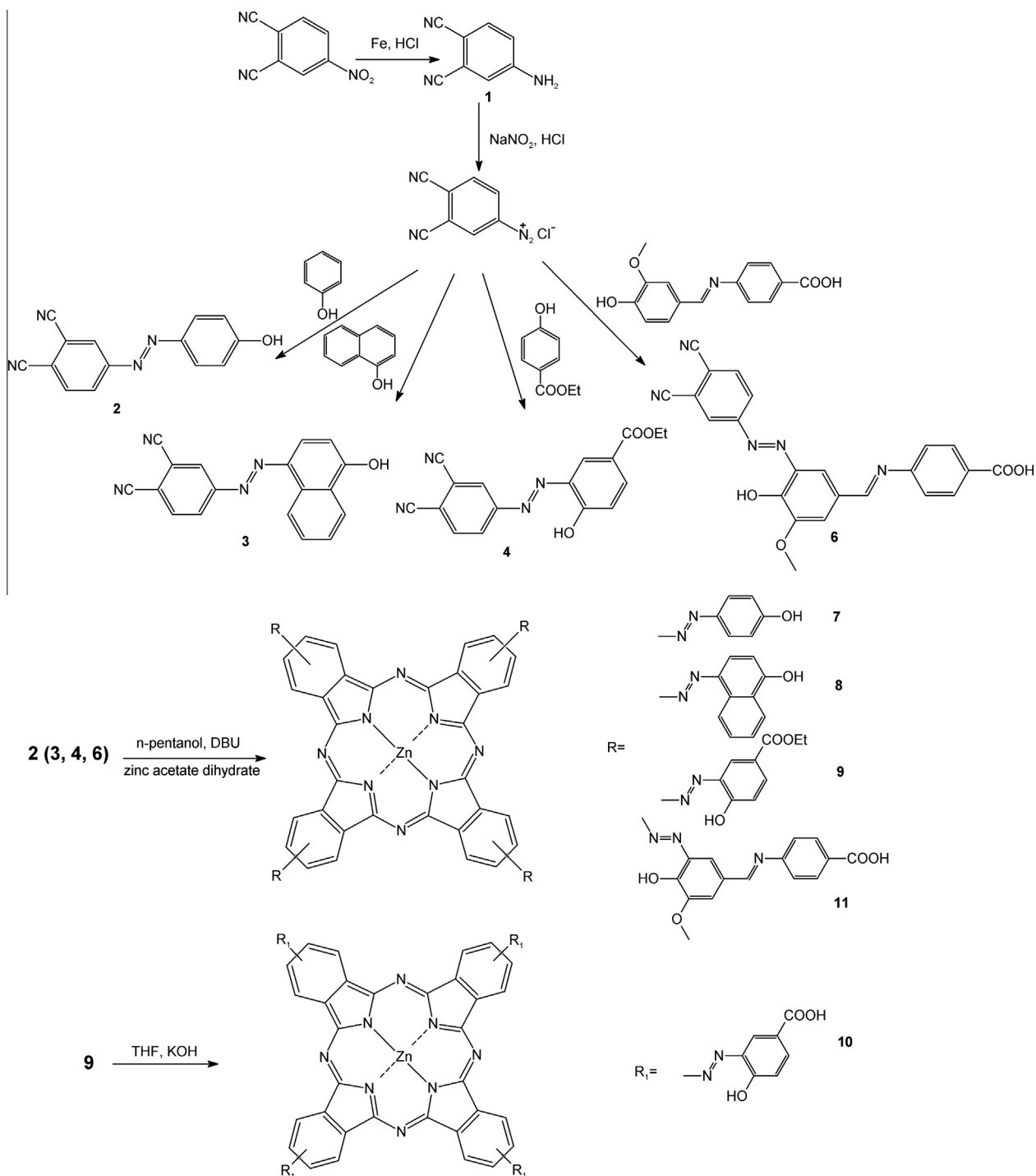
The synthetic routes to the azo-coupled phthalocyanines (**7**, **8**, **10** and **11**) were given in Scheme 1. The first step was the synthesis of 4-aminophthalonitrile **1**. This was reduced from 4-nitrophthalonitrile using Fe powders and concentrated hydrochloric acid in deionized water. 4-Aminophthalonitrile was used to prepare the diazonium salt solutions to synthesize the four azo-phthalonitriles: 4-(4-hydroxyphenylazo)phthalonitrile **2**, 4-(4-hydroxy-naphthalen-1-ylazo) phthalonitrile **3**, 4-(2-hydroxyl-5-ethyl-oxycarbonyl-phenylazo)phthalonitrile **4** and 4-[2-hydroxyl-3-methoxyl-4-(4-carboxyl-benzylidene-amino)phenylazo]phthalonitrile **6**. The coupling between the arenediazonium ion and phenol derivatives was via electrophilic aromatic substitution reactions. The arenediazonium ion reacted as an electrophilic reagent, but it was so mild that only highly activated rings could be used. For this reason, the coupling reactions were carried out in alkali medium to activate the phenolic hydroxyl groups. The purification of the four azo-coupled phthalonitriles was achieved by recrystallization. The solubility of the four azo-phthalonitriles was good in common organic solvents, such as alcohol and ethyl acetate. The synthesis of the four azo-coupled phthalonitrile compounds was the most important step in these reaction sequences.

The template self-cyclotetramerization of the azo-coupled phthalonitriles **2**, **3**, **4** and **6** in the high-boiling solvent n-pentanol under a nitrogen atmosphere afforded the four azo-coupled zinc phthalocyanines **7**, **8**, **9** and **11**, respectively. Hydrolysis of **9** with potassium hydroxide and acidification with hydrochloric acid gave **10** [30]. The basicity of DBU was so sufficient that ester exchange between ethyl ester and n-butanol inevitably occurred [9]. Therefore, compound **9** was actually a mixture of the ethyl and n-butyl esters. However, no further subtle purification, such as chromatography, towards **9** was needed before further hydrolysis. The purification of the four metal phthalocyanines was carried out by Soxhlet extraction. All the finely washed azo-coupled phthalocyanines were fine black powders. Compounds **7**, **8**, **10** and **11** were slightly soluble in common organic solvents, such as alcohol and ethyl acetate, but exhibited good solubility in Py (pyridine), THF, DMF and DMSO.

The structures of the target compounds were characterized by elemental analysis together with spectral data (FT-IR,  $^1H$  NMR, mass and UV-Vis). The characterization data of the new compounds were consistent with the assigned formula.

According to FT-IR spectroscopy data, the formation of compound **1** was clearly confirmed by the disappearance of the  $NO_2$  bands at 1540 and 1360  $cm^{-1}$ , and the appearance of  $NH_2$  bands at 3446 and 3357  $cm^{-1}$ . For the four azo-coupled phthalonitriles **2**, **3**, **4** and **6**, the characteristic vibrations corresponding to  $C\equiv N$  were at 2242, 2226, 2236 and 2231  $cm^{-1}$ , respectively. The  $N=N$  vibrations for **2–4** and **6** were observed at 1460, 1482, 1446 and 1508  $cm^{-1}$ , respectively. The IR spectra of compounds **2** and **3** showed sharp OH bands at 3339 and 3259  $cm^{-1}$ , while compounds **4** and **6** showed broad OH bands at 3221 and 3374  $cm^{-1}$  due to stronger intramolecular hydrogen bonding between the OH group and nitrogen atom in the azo groups. IR spectra of compounds **5** and **6** showed aromatic  $CH=N$  peaks at 1593 and 1599  $cm^{-1}$ . A characteristic substituted naphthalene peak at about 758  $cm^{-1}$  for the azo-coupled phthalonitrile compound **3** was observed as well [15].

For the  $^1H$  NMR spectra of compounds **2–6**, aromatic protons appeared at 6.91–8.41, 6.89–8.42, 7.64–8.39, 6.65–8.13 and 7.16–8.44 ppm, respectively. The hydroxyl protons of compounds **2–6** showed singlet peaks at 10.41, 10.27, 9.44, 9.57 and 10.24 ppm,



**Scheme 1.** Synthetic routes for the four azo-coupled phthalonitriles (**2**, **3**, **4** and **6**) and their corresponding zinc phthalocyanines (**7**, **8**, **9**, **10** and **11**).

respectively. The presence of hydrogen bonds between the OH group and the nitrogen atom in azo groups led to resonances of hydroxyl protons occurring in the range 9–11 ppm [13]. The <sup>1</sup>H NMR spectra of compounds **5** and **6** showed resonances of protons belonging to the Schiff base groups at 8.35 and 8.41 ppm. In addition, elemental analysis results of compounds **2–6** were good agreement with the proposed structures.

After cyclotetrimerization, the sharp peaks for the C≡N vibrations completely disappeared in the FT-IR spectra [31]. The IR spectra of all the azo-coupled phthalocyanines featured Pc ring vibration peaks at around 1600 cm<sup>-1</sup> (CH=N) and 1500 cm<sup>-1</sup>

(C=C) as expected. The <sup>1</sup>H NMR spectra of the four substituted azo-phthalocyanines were almost identical with those of the starting compounds **2**, **3**, **4** and **6** except for broadening and small shift due to the existence of statistical isomers and possible aggregation at the measured concentration [32]. For compounds **9** and **11**, the integral ratio of the aromatic protons to aliphatic protons was similar to the corresponding phthalonitrile compounds. For the <sup>1</sup>H NMR spectrum of compound **10**, the resonance belonging to the carboxyl protons showed a singlet peaks at 12.73 ppm, clearly confirming the hydrolysis of the ester groups. The disappearance of the resonances of the aliphatic protons of **9** also confirmed the hydro-

lysis. In the mass spectra of the five azo-coupled phthalocyanines, the molecular ion peaks, which were observed at  $m/z$ : 1058.62 [ $M^+$ ] for **7**, 1258.41 [ $M^+$ ] for **8**, 1346.87 [ $M^+$ ] for **9**, 1234.69 [ $M^+$ ] for **10** and 1767.21 [ $M^+$ ] for **11**, supported the desired structures. In addition, the elemental analysis was satisfactory.

### 3.2. Absorption properties

The electronic absorption spectra of the phthalonitrile precursors **2**, **3**, **4** and **6** were recorded in THF solution and the azo-coupled zinc phthalocyanines **7**, **8**, **10** and **11** were tested both in THF solution and adsorbed on anatase  $TiO_2$  thin films. Figs. 1–4 show the absorption spectra of the unsubstituted zinc phthalocyanine (Zn<sup>I</sup>Pc), the phthalonitrile precursors **2**, **3**, **4** and **6** (both as reference compounds) and the azo-coupled phthalocyanines. The UV–Vis spectra of the azo-coupled phthalocyanines showed the characteristic Q-bands. The Q-band absorptions of the azo-coupled zinc phthalocyanines **7**, **8**, **10** and **11** were observed as single high intensity bands due to  $\pi \rightarrow \pi^*$  transitions at 718, 740, 716 and 729 nm, respectively. For compounds **8** and **11**, the B-band, usually located at 350 nm for the normal Pcs, were replaced by strong and broad new absorption bands appearing at approximately 300–600 nm, however for compounds **7** and **10**, the B-band were clear and located at 376 and 362 nm, respectively. The above phenomena are closely related to increased expansion of the  $\pi$ -conjugation of the dyes due to the introduced azo moieties, and this could also be used to illustrate the red shift of the Q-bands of four azo-coupled phthalocyanines. The absorptions in the spectral window between 400 and 600 nm of the four azo-coupled phthalocyanines were remarkable, and these were caused by efficient electron transfer from the azobenzene  $\pi^*$  orbital to the Pc  $S_1$  level [30]. Additional absorptions of this kind are scarce and would make Pcs acquire novel opto-electronic properties and collect panchromatic photoelectrons efficiently. It is clear that the absorption characteristics of both azobenzene and Pc moieties are displayed when conjugated into one molecule.

The absorption spectra of the azo-coupled zinc phthalocyanines **7**, **8**, **10** and **11** adsorbed onto 6  $\mu m$  thick  $TiO_2$  films were similar to those of the solution spectra, but exhibited a small red shift and the bands were much broader. This may be due to the presence of anchoring group protons, which on adsorption on  $TiO_2$  release the proton and bind to  $Ti^{4+}$ . The  $Ti^{4+}$  acts as electron withdrawing and produces a red shift in the absorption bands [33,34]. In addition, light scattering and re-absorption from the nanoparticle surface of  $TiO_2$  may also lead to the spectra significantly broadening. The large coverage of the solar spectrum from UV to near IR region renders these phthalocyanines ideal light-harvesting materials in organic solar cells.

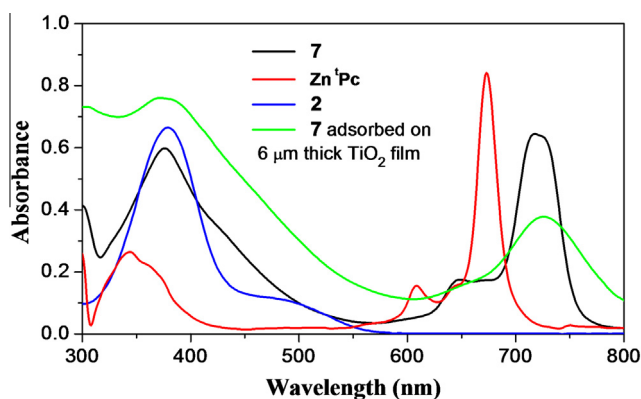


Fig. 1. UV–Vis absorption spectra of **7**, Zn<sup>I</sup>Pc and **2** in THF at  $1 \times 10^{-5}$  M and **7** adsorbed on a 6  $\mu m$  thick  $TiO_2$  film.

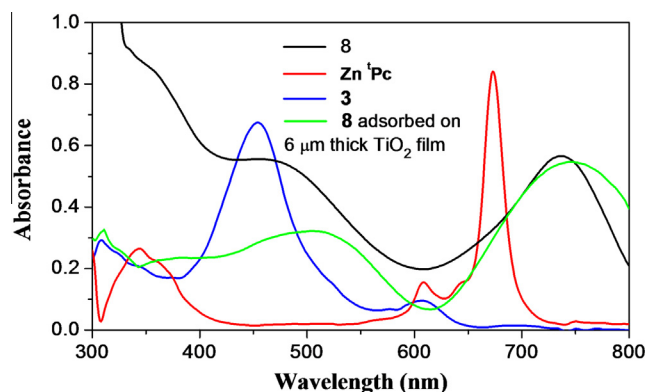


Fig. 2. UV–Vis absorption spectra of **8**, Zn<sup>I</sup>Pc and **3** in THF at  $1 \times 10^{-5}$  M and **8** adsorbed on a 6  $\mu m$  thick  $TiO_2$  film.

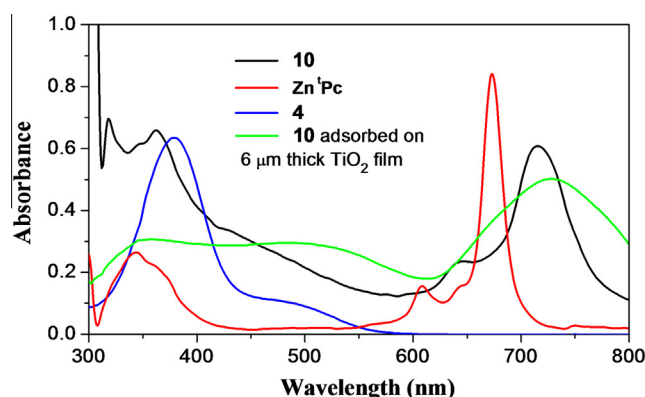


Fig. 3. UV–Vis absorption spectra of **10**, Zn<sup>I</sup>Pc and **4** in THF at  $1 \times 10^{-5}$  M and **10** adsorbed on a 6  $\mu m$  thick  $TiO_2$  film.

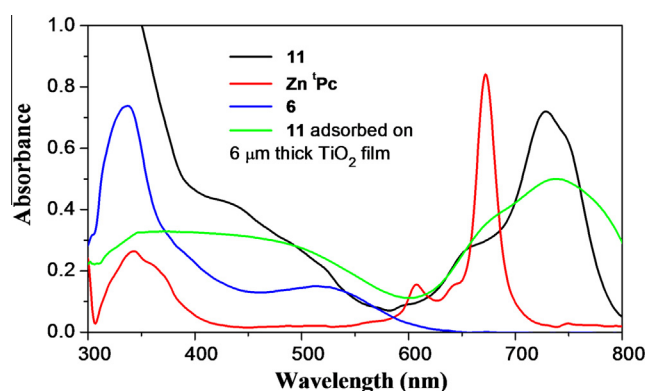


Fig. 4. UV–Vis absorption spectra of **11**, Zn<sup>I</sup>Pc and **6** in THF at  $1 \times 10^{-5}$  M and **11** adsorbed on a 6  $\mu m$  thick  $TiO_2$  film.

The optical energy band gaps ( $E_g^{opt}$ ) of **7**, **8**, **10** and **11** were estimated according to the following equation [35]:

$$E_g^{opt} = \frac{hc}{\lambda_{max}} = \frac{1240}{\lambda_{max}}$$

where  $\lambda_{max}$  is the absorption maximum.

The UV–Vis data and  $E_g^{opt}$  energies estimated from the absorption maxima of Zn<sup>I</sup>Pc, **7**, **8**, **10** and **11** are shown in Table 1. The decrease of the energy gaps between the HOMO and LUMO compared to Zn<sup>I</sup>Pc results in the red shift of the absorption bands of the dyes.

**Table 1**

The UV–Vis data in THF and  $E_g^{\text{opt}}$  energy values of Zn<sup>I</sup>Pc and azo-coupled phthalocyanines **7**, **8**, **10** and **11**.

Comp.	$\lambda_{\text{max}}$ , nm (log $\epsilon$ ) <sup>a</sup>		$E_g^{\text{opt}}$ (eV) <sup>b</sup>
	B band	Q band	
Zn <sup>I</sup> Pc	344 (4.42)	608 (4.19), 673 (4.92)	1.84
<b>7</b>	376 (4.78)	649 (4.24), 718 (4.72)	1.72
<b>8</b>	–	740 (4.77)	1.67
<b>10</b>	362 (4.82)	647 (4.37), 716 (4.78)	1.73
<b>11</b>	–	664 (4.46), 729 (4.86)	1.70

<sup>a</sup> The solvent is THF.

<sup>b</sup> The optical energy gaps from the UV–Vis absorption spectra.

### 3.3. Electrochemical properties

Cyclic voltammetry experiments were carried out at room temperature under nitrogen against a saturated calomel electrode (SCE) in THF containing 0.1 M tetrabutylammonium perchlorate (TBPA) on a Pt working electrode to study the electrochemical behaviors of the four azo-coupled zinc phthalocyanines. The cyclic voltammograms of the four compounds are illustrated in Fig. 5. Compounds **7**, **8**, **10** and **11** showed similar single reversible reduction peaks attributed to the reduction of the four azobenzene moieties at  $-0.98$ ,  $-1.01$ ,  $-1.05$  and  $-1.13$  V, respectively. At the same time, the CV scans of **7**, **8** and **10** showed similar quasi-reversible oxidation waves at 0.67, 0.52 and 0.54 V, and **11** showed an irreversible oxidation wave at 0.55 V. This was ascribed to the oxidation of the Pc rings [30].

The lowest unoccupied molecular orbital (LUMO) of the dye is closely related with the electron injection efficiency of the TiO<sub>2</sub> surface. Additionally, the highest occupied molecular orbital (HOMO) of the sensitizer should lie below the energy level of the I<sub>3</sub><sup>-</sup>/I<sup>-</sup> redox couple to achieve efficient regeneration of the oxidized dyes formed after electron injection [3]. The HOMO–LUMO levels of the azo-coupled zinc phthalocyanines **7**, **8**, **10** and **11** were estimated through the equation reported by de Leeuw et al. [36]:

$$E_{\text{HOMO}} = -\left(E_{\text{onset-SCE}}^{\text{Oxy}} + 4.4 \text{ eV}\right)$$

$$E_{\text{LUMO}} = -\left(E_{\text{onset-SCE}}^{\text{Red}} + 4.4 \text{ eV}\right)$$

$E_{\text{onset-SCE}}^{\text{Oxy}}$  and  $E_{\text{onset-SCE}}^{\text{Red}}$  indicate the onset values of the oxidation and reduction potentials.

The LUMO energy levels of compounds **7**, **8**, **10** and **11** were found to be  $-3.0$ ,  $-2.97$ ,  $-2.95$  and  $-2.94$  eV, respectively. The HOMO energy levels of compounds **7**, **8**, **10** and **11** were found to be  $-4.75$ ,  $-4.65$ ,  $-4.72$  and  $-4.73$  eV, respectively. Band gap values from the electrochemically determined data were 1.75, 1.68, 1.77 and 1.79 eV, respectively. All the data are listed in Table 2. Compared with the energy gap calculated from the UV–Vis absorption spectra, the band gap values read from the CV graphs are larger. This is probably due to the interface dipole effect on modifying the energy barriers between the electrodes and the organic materials [37]. However, the energy gap values read from the CV graphs on the whole correlate well with the calculated values from the absorption spectra.

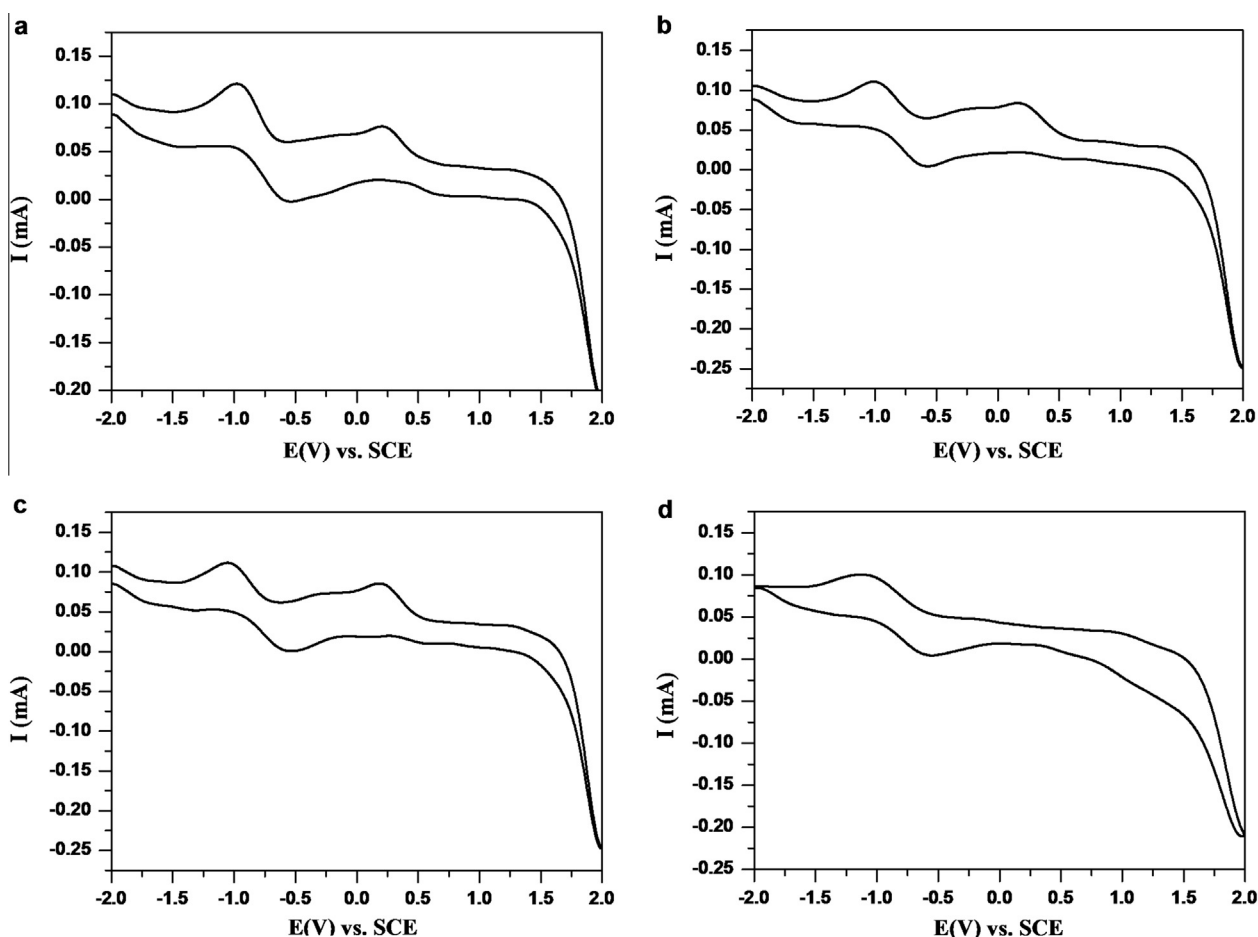


Fig. 5. Cyclic voltammograms of azo-coupled phthalocyanines **7** (a), **8** (b), **10** (c) and **11** (d). Medium = THF containing 0.1 M TBPA. Scan rate = 100 mV s<sup>-1</sup>.

We took the previously reported zinc phthalocyanine sensitizer TT1 [7] as a reference for assessing the LUMO levels of the sensitizers **7**, **8**, **10** and **11**. TT1 showed 80% IPCE (incident photon-to-current conversion efficiency) at 690 nm and a record  $\eta$  value of 3.5%. The LUMO level of TT1 was ca.  $-3.17$  eV [38], which is relatively low, a comparative shortcoming for the further improvement of  $\eta$  values of phthalocyanine-sensitized solar cells. As observed in Table 2, the four azo-coupled phthalocyanines have higher LUMO energy levels than TT1, indicating that the four compounds could be promising for providing higher electron injection efficiencies and  $\eta$  values. Also, as it was difficult to estimate the theoretical redox potential of the electrolyte, we choose the reported dye N3 [39] as a reference to assess the HOMO level of the four azo-coupled phthalocyanines. N3 is a famous ruthenium-polypyridyl sensitizer with a HOMO energy level of ca.  $-5.08$  eV [38]. A sensitizer with a HOMO level close to or higher than that of N3 might be promising for regeneration since N3 can be regenerated well. The HOMO levels of the four azo-coupled phthalocyanines were higher than N3 so that the regeneration of four compounds by iodide is thermodynamically favorable.

### 3.4. Thermal properties

The thermal properties of **7**, **8**, **10** and **11** were tested by using TGA under a nitrogen atmosphere. For roof top applications of dye-sensitized solar cells, the thermal stability of organic dyes adsorbed on nanocrystalline TiO<sub>2</sub> is very essential.

The thermogravimetric curves for the four azo-coupled phthalocyanines are shown in Fig. 6. From the curves, minor decomposition reactions occurred at 295, 240, 270 and 230 °C for compounds **7**, **8**, **10** and **11**, respectively, with a weight loss of 22%, 3%, 10% and 11%. This stage corresponded to the partial degradation of the aromatic substituents introduced onto the Pc ring. Major decomposition reactions occurred at 400, 450, 390 and 370 °C for **7**, **8**, **10** and **11** and the corresponding weight losses were 27%, 30%, 42% and 33%, respectively. This stage corresponded to the degradation of

the N=N bond and breakage of the bonds between Zn and the Pc ring [40,41]. It was seen that **10** and **11** had the lowest major decomposition temperature among the four azo-coupled phthalocyanines. This might be due to the existence of carboxyl groups and Schiff base groups in the structures of **10** and **11**. From the TGA curves, we also found that the removal of carboxyl groups and decomposition of the Schiff base structures led to the weight loss onset for **10** and **11** at 300 °C, compared to higher onset temperatures for **7** and **8**. Generally, the thermal data imply that **7** and **8** have better stability and also agree with the structures of the four azo-coupled phthalocyanines.

### 3.5. Photovoltaic performances

The performances of DSSCs are characterized primarily by the open-circuit voltage ( $V_{oc}$ ), short-circuit photocurrent density ( $J_{sc}$ ), photocurrent/voltage curve ( $J/V$  curve), incident photon-to-current conversion efficiency (IPCE), fill factor (ff) and solar energy-to-electricity conversion yield ( $\eta$ ) [3]. The IPCE is directly related to the absorption properties of the dye, the amount of adsorbed dyes on the TiO<sub>2</sub> surface, the amount of electron injection from the photo-excited dye to the CB of the TiO<sub>2</sub> and the efficiency of the collection of electrons in the external circuit, and it can be represented by the following equation:

$$\text{IPCE (\%)} = \frac{1240(\text{eV nm})J_{ph}(\text{mA cm}^{-2})}{\lambda(\text{nm})I(\text{mW cm}^{-2})} \quad (1)$$

$J_{ph}$  is the short-circuit photocurrent density generated by monochromatic light,  $\lambda$  and  $I$  are the wavelength and the intensity of the monochromatic light, respectively.

The fill factor is defined as the maximum power output of the solar cell per unit area divided by the product of  $J_{sc}$  and  $V_{oc}$ . The fill factor can be represented by the following equation:

$$\text{ff} = \frac{P_{\max}}{J_{sc}V_{oc}} \quad (2)$$

The solar energy-to-electricity conversion yield  $\eta$  is defined as the ratio of the maximum output electrical power of the DSSC to the energy of the incident sunlight ( $I_0$ ). The  $\eta$  value can be calculated from the following equation:

$$\eta (\%) = \frac{J_{sc}(\text{mA cm}^{-2})V_{oc}(\text{V})\text{ff}}{I_0(\text{mW cm}^{-2})} \quad (3)$$

To judge the potential of the newly synthesized azo-coupled zinc phthalocyanines **7**, **8**, **10** and **11** as sensitizers for DSSC, P25 TiO<sub>2</sub> films were used to evaluate their photovoltaic performances. TiO<sub>2</sub> electrodes (6  $\mu\text{m}$  thick) were sensitized with the four azo-coupled phthalocyanines. The photovoltaic characterization data for sensitizer dyes **7**, **8**, **10** and **11** are summarized in Table 3. The photocurrent–voltage curves ( $J$ – $V$  curves) of the four azo-coupled phthalocyanines sensitized TiO<sub>2</sub> cells are depicted in Fig. 7. We have observed that the power conversion efficiencies ( $\eta$ ) for compounds

**Table 2**  
Electrochemical properties of the azo-coupled phthalocyanines **7**, **8**, **10** and **11**.

Comp.	$E_{ox}/E_{red}$ (V) <sup>a</sup>	LUMO (eV)	HOMO (eV)	$E_g$ (eV) <sup>b</sup>
<b>7</b>	0.35/–1.40	–3.00	–4.75	1.75
<b>8</b>	0.25/–1.43	–2.97	–4.65	1.65
<b>10</b>	0.32/–1.45	–2.95	–4.72	1.77
<b>11</b>	0.33/–1.46	–2.94	–4.73	1.79

<sup>a</sup> Onset voltages from CV curves.

<sup>b</sup> Energy gaps from the electrochemically determined values.

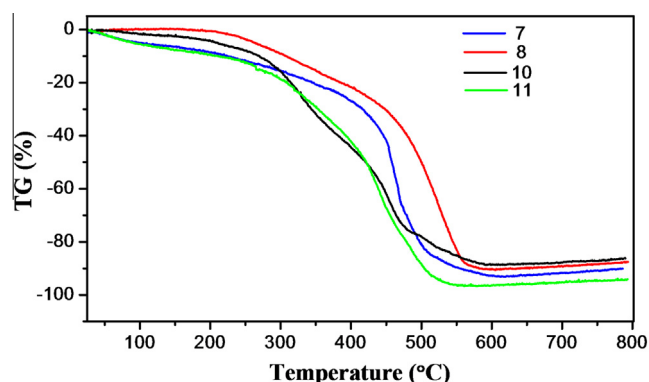


**Fig. 6.** TG curves of compounds **7**, **8**, **10** and **11** with a heating rate of  $10\text{ °C min}^{-1}$  under nitrogen.

**Table 3**  
Photovoltaic characteristics of DSSCs<sup>a</sup> with the azo-coupled phthalocyanine dyes **7**, **8**, **10** and **11** under one-sun conditions and values of the IPCE.

Comp.	$J_{sc}$ (mA cm <sup>-2</sup> )	$V_{oc}$ (V)	ff	$\eta$ (%)	IPCE <sub>max</sub> (%)
<b>7</b>	3.5	0.54	0.74	1.4	41
<b>8</b>	6.6	0.59	0.69	2.7	49
<b>10</b>	4.4	0.56	0.72	1.8	45
<b>11</b>	5.2	0.57	0.70	2.1	46

<sup>a</sup> The TiO<sub>2</sub> electrode was sensitized with  $1 \times 10^{-4}$  M sensitizer. The electrolyte was 0.05 M iodine and 0.5 M LiI in acetonitrile. The thickness and area of TiO<sub>2</sub> were 6  $\mu\text{m}$  and 0.68 cm<sup>2</sup>, respectively.

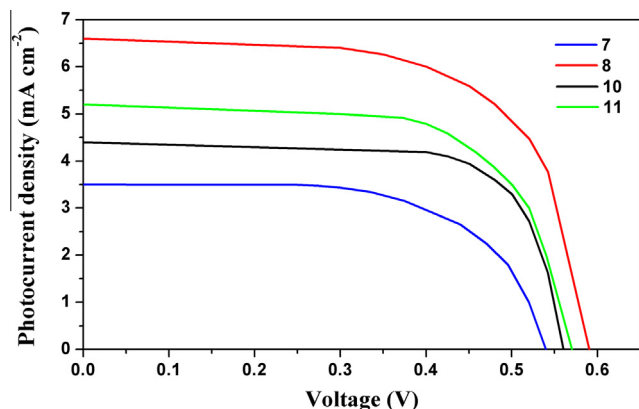


Fig. 7. Photocurrent–voltage curves of the azo-coupled phthalocyanine dyes **7**, **8**, **10** and **11**.

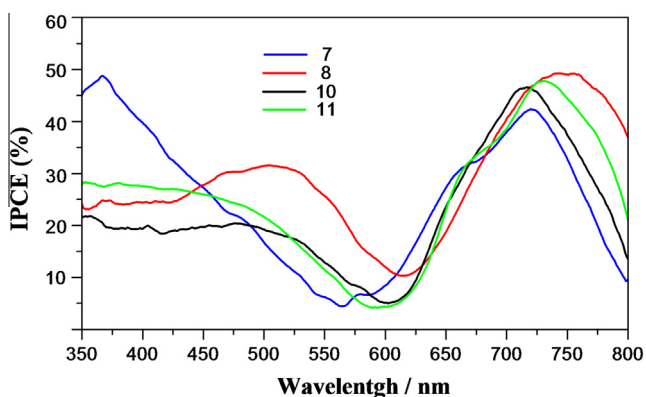


Fig. 8. IPCEs of dye-sensitized solar cells with the four different azo-coupled phthalocyanine dyes.

**7**, **8**, **10** and **11** sensitized TiO<sub>2</sub> cells were 1.4%, 2.7%, 1.8% and 2.1%, respectively. The compound **8** sensitized cell exhibited a maximum  $\eta$  value of 2.7%,  $J_{sc} = 6.6 \text{ mA cm}^{-2}$ ,  $V_{oc} = 0.59 \text{ V}$  and  $ff = 0.69$ . The result was closely related to the broader absorptions and the weak tendency of aggregation due to higher steric hindrance of the four naphthol groups compared to the other three compounds. Compounds **7** and **10** have similar  $\pi$  conjugated structures, however, the  $\eta$  value of compound **10** sensitized cell was 1.8% ( $J_{sc} = 4.4 \text{ mA cm}^{-2}$ ,  $V_{oc} = 0.56 \text{ V}$  and  $ff = 0.72$ ), which was higher than that of the dye **7** sensitized cell ( $\eta = 1.4\%$ ,  $J_{sc} = 3.5 \text{ mA cm}^{-2}$ ,  $V_{oc} = 0.54 \text{ V}$  and  $ff = 0.74$ ). This may be due to the four carboxyl groups of compound **8**, which could provide a stronger ester linkage with the TiO<sub>2</sub> surface and better electron communication.

To investigate the photovoltaic performances of the present cells in more detail, the photocurrent action spectra of dyes **7**, **8**, **10** and **11** sensitized TiO<sub>2</sub> cells were measured. The photocurrent action spectra are shown in Fig. 8. It was found that the photocurrent response resembled the absorption spectra, except for a slight red shift by ca. 10 nm. The absorption of the azo moieties made the photo-response of the four azo-coupled phthalocyanine thin films display broad and intense spectral responses, extending from 350 to 800 nm. The maximal IPCE values at the near-infrared region were measured to be 41%, 49%, 45% and 46% for compounds **7**, **8**, **10** and **11**, respectively.

#### 4. Conclusions

In summary, we have designed, synthesized and characterized four symmetrical azo-coupled zinc phthalocyanines (**7**, **8**, **10** and **11**) with hydroxyl or carboxyl anchoring groups, which have incor-

porated two spectrally complementary photogenerators (azo dyes and Pcs) by N=N double bonds in single structures. Compared with the phthalocyanines where azo moieties were introduced through oxygen bridges, the four compounds showed impressive absorptions and photocurrent responses in the visible and near-IR regions as a result of lowering of energy gaps. Electrochemical studies were made to investigate the HOMO and LUMO levels. The LUMO levels of the four sensitizers were high enough to achieve efficient electron injection from the excited dyes to the conduction band of TiO<sub>2</sub>. In addition, the HOMO levels of the four dyes could ensure efficient regeneration of the oxidized dyes. The four azo-coupled phthalocyanines were tested in DSSC. The low efficiency of DSSC using the four azo-coupled phthalocyanines is probably due to aggregation of the azo-coupled phthalocyanine molecules on the TiO<sub>2</sub> surface and the symmetrical structures of the four dyes, which are not good enough for intramolecular charge transfer and directional electron injection. Thermal stability studies showed that the four sensitizers were stable above 200 °C.

#### Acknowledgments

The authors would like to acknowledge financial support from the National Nature Science Foundation of China (Grant number: 51272239) and the Shanxi Natural Science Foundation (Grant number: 2011011022-4).

#### Appendix A. Supplementary data

Supplementary data associated with this article can be found, in the online version, at <http://dx.doi.org/10.1016/j.poly.2014.10.026>. These data include MOL files and InChIKeys of the most important compounds described in this article.

#### References

- [1] A. Hagfeldt, G. Boschloo, L. Sun, L. Kloo, H. Pettersson, *Chem. Rev.* **110** (2010) 6595.
- [2] N. Yeh, P. Yeh, *Renew. Sustain. Energy Rev.* **21** (2013) 421–431.
- [3] Y. Ooyama, Y. Harima, *Eur. J. Org. Chem.* (2009) 2903.
- [4] A. Mishra, M.K.R. Fischer, P. Bäuerle, *Angew. Chem., Int. Ed.* **48** (2009) 2474.
- [5] C.C. Leznoff, A.B.P. Lever, *Phthalocyanines Properties and Applications*, vol. 1–4, VCH, Weinheim, 1989–1996.
- [6] V.N. Nemykin, E.A. Lukyanets, *ARKIVOC* **1** (2010) 136.
- [7] J.J. Cid, J.H. Yum, S.R. Jang, M.K. Nazeeruddin, E. Martínez-Ferrero, E. Palomares, J. Ko, M. Grätzel, T. Torres, *Angew. Chem., Int. Ed.* **46** (2007) 8358.
- [8] S. Mori, M. Nagata, Y. Nakahata, K. Yasuta, R. Goto, M. Kimura, M. Taya, *J. Am. Chem. Soc.* **132** (2010) 4054.
- [9] S. Eu, T. Katoh, T. Umeyama, Y. Matano, H. Imahori, *Dalton Trans.* (2008) 5476.
- [10] L. Giribabu, V.K. Singh, C.V. Kumar, Y. Soujanya, P.Y. Reddy, M.L. Kantam, *Sol. Energy* **85** (2011) 1204.
- [11] F. Liang, F. Shi, Y. Fu, L. Wang, X. Zhang, Z. Xie, Z. Su, *Sol. Energy Mater. Sol. Cells* **94** (2010) 1803.
- [12] M. Pişkin, M. Durmuş, M. Bulut, *Inorg. Chim. Acta* **373** (2011) 107.
- [13] C. Kantar, F. Mert, S. Şaşmaz, *J. Organomet. Chem.* **696** (2011) 3006.
- [14] N. Zharnikova, N. Usol'tseva, E. Kudrik, M. Thelakkat, *J. Mater. Chem.* **19** (2009) 3161.
- [15] H.Y. Yenilmez, A. Okur, A. Gül, *J. Organomet. Chem.* **692** (2007) 940.
- [16] T. Muto, T. Temma, M. Kimura, K. Hanabusa, H. Shirai, *J. Org. Chem.* **66** (2001) 6109.
- [17] C. Farren, C.A. Christensen, S. Fitzgerald, M.R. Bryce, A. Beeby, *J. Org. Chem.* **67** (2002) 9130.
- [18] C.A. Barker, X. Zeng, S. Bettington, A.S. Batsanov, M.R. Bryce, A. Beeby, *Chem. Eur. J.* **13** (2007) 6710.
- [19] X. Li, L.E. Sinks, B. Rybtchinski, M.R. Wasielewski, *J. Am. Chem. Soc.* **126** (2004) 10810.
- [20] N. Nombona, T. Nyokong, *Dyes Pigm.* **80** (2009) 130.
- [21] G. Hallas, A.D. Towns, *Dyes Pigm.* **33** (1997) 319.
- [22] G. Hallas, A.D. Towns, *Dyes Pigm.* **35** (1997) 219.
- [23] A.D. Towns, *Dyes Pigm.* **42** (1999) 3.
- [24] M.S. Ho, A. Natansohn, *Macromolecules* **28** (1995) 6124.
- [25] F. Chami, M.R. Wilson, *J. Am. Chem. Soc.* **132** (2010) 7794.
- [26] F. Borbone, A. Carella, L. Ricciotti, A. Tuzi, A. Roviello, A. Barsella, *Dyes Pigm.* **88** (2011) 290.
- [27] D.D. Perrin, W.L.F. Armarego, *Purification of Laboratory Chemicals*, second ed., Pergamon Press, Oxford, 1989.

- [28] Y.G. Kim, Z.A. Akbar, D.Y. Kim, S.M. Jo, S.Y. Jang, *Appl. Mater. Interfaces* 5 (2013) 2053.
- [29] X. Zhang, M. Wang, H. He, L. Mao, *Asian J. Chem.* 26 (2014) 2229.
- [30] Y. Liu, H. Lin, X. Li, J. Li, H. Nan, *Inorg. Chem. Commun.* 13 (2010) 187.
- [31] M.S. Ağırtaş, *Inorg. Chim. Acta* 360 (2007) 2499.
- [32] H.T. Akçay, M. Pişkin, Ü. Demirbaş, R. Bayrak, M. Durmuş, E. Menteşe, H. Kantekin, *J. Organomet. Chem.* 745–746 (2013) 379.
- [33] M.K. Nazeeruddin, R. Splivallo, P. Liska, P. Comte, M. Grätzel, *Chem. Commun.* (2003) 1456.
- [34] J.H. Yum, S. Jang, R. Humphry-Baker, M. Grätzel, J.J. Cid, T. Torres, M.K. Nazeeruddin, *Langmuir* 24 (2008) 5636.
- [35] D. Zhang, X. Zhang, L. Zhang, L. Mao, *Bull. Korean Chem. Soc.* 33 (2012) 1225.
- [36] D.M. de Leeuw, M.M.J. Simenon, A.R. Brown, R.E.F. Einerhand, *Synth. Met.* 87 (1997) 53.
- [37] S. Janietz, D.D.C. Bradley, M. Grell, C. Giebeler, M. Inbasekaran, E.P. Woo, *Appl. Phys. Lett.* 73 (1998) 2453.
- [38] L. Yang, L. Guo, Q. Chen, H. Sun, J. Liu, X. Zhang, X. Pan, S. Dai, *J. Mol. Graphics Modell.* 34 (2012) 1.
- [39] M.K. Nazeeruddin, A. Kay, I. Rodicio, R. Humphry-Baker, E. Müller, P. Liska, N. Vlachopoulos, M. Grätzel, *J. Am. Chem. Soc.* 115 (1993) 638.
- [40] H. Dinçalp, F. Toker, İ. Durucasu, N. Avcıbaş, S. İcli, *Dyes Pigm.* 75 (2007) 11.
- [41] R. Seoudi, G.S. El-Bahy, Z.A. El Sayed, *J. Mol. Struct.* 753 (2005) 119.